

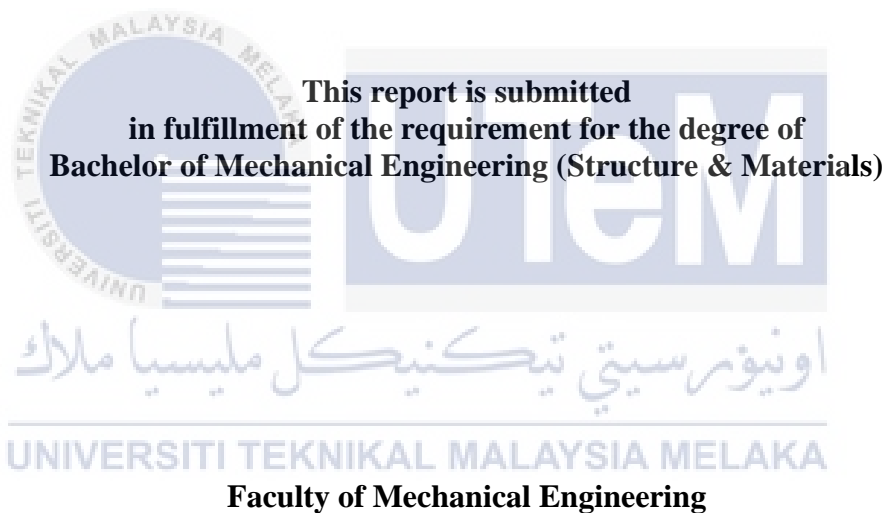
**THE PERFORMANCE OF STRETCHABLE CONDUCTIVE INK (SCI) UNDER
MECHANICAL FACTOR**



UNIVERSITI TEKNIKAL MALAYSIA MELAKA

**THE PERFORMANCE OF STRETCHABLE CONDUCTIVE INK (SCI)
UNDER MECHANICAL FACTOR**

MUHAMMAD IZWAN BIN ABDUL RAHIM



UNIVERSITI TEKNIKAL MALAYSIA MELAKA

JANUARY 2022

DECLARATION

I declare that this project report entitled “The Performance of Stretchable Conductive Ink (SCI) Under Mechanical Factor” is the result of my own work except as cited in the references

Signature :

Name :

Date :



اونيورسيتي تيكنيكل مليسيا ملاك

UNIVERSITI TEKNIKAL MALAYSIA MELAKA

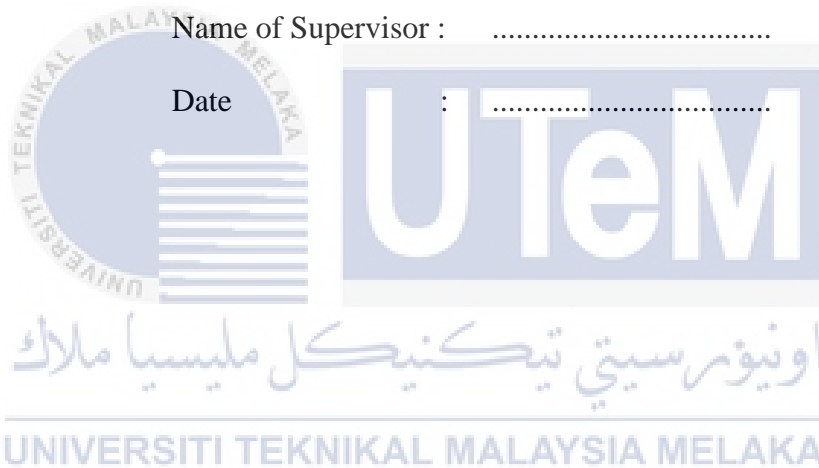
APPROVAL

I hereby declare that I have read this project report and in my opinion this report is sufficient in terms of scope and quality for the award of the degree of Bachelor of Mechanical Engineering (Structure & Materials).

Signature :

Name of Supervisor :

Date :



DEDICATION

To my beloved mother and father



ABSTRACT

Graphene Nanoplatelets (GNPs) are excellent electrical and mechanical fillers for conductive polymers. However, the GNP size might affect the conductive polymer's conductivity and reliability, especially when it is subjected to various types of loading. This study shows the effect of GNP particle size on conductivity and reliability of conductive polymer composites when subjected to mechanical fatigue stress through the stretch test. In this work, two types of GNP filler sizes are considered which is the 5 μ m and 15 μ m with a mixed of surfactant. Following the manual cyclic stretch test, the results show that the resistivity increases as the number of cycles increases due to cracks' formation. The zero reading of bulk resistivity of 5 μ m and 15 μ m particles size was obtained when the stretch reached approximately 13 cm to 14 cm in length, which is 225% to 250% of the strain percentage. The applicable elongation of both particle sizes to withstand longer with better bulk resistivity is 125% with an elongation of 0.5 cm from the initial length of 4.0 cm. 15 μ m. Other than that, it was found that the peel strength of 15 μ m GNP which is 0.00419 N/mm is better compared to 5 μ m GNP which is 0.00328 N/mm. The surface morphology of each particle was described as a result of its bulk resistivity after being stretched through the cycles.

اونيور سیتی تکنیکل ملیسیا ملاک

UNIVERSITI TEKNIKAL MALAYSIA MELAKA

ABSTRAK

Graphene nanoplatelets (GNPs) adalah pengisi elektrik dan mekanikal yang sangat baik untuk polimer konduktif. Walau bagaimanapun, saiz GNP mungkin menjejaskan kekonduksian dan kebolehpercayaan polimer konduktif, terutamanya apabila ia tertakluk kepada pelbagai jenis beban. Kajian ini menunjukkan kesan saiz zarah GNP pada kekonduksian dan kebolehpercayaan komposit polimer konduktif apabila tertakluk kepada tekanan keletihan mekanikal melalui ujian regangan. Dalam kajian ini, dua jenis saiz pengisi GNP dipertimbangkan iaitu 5 μ m dan 15 μ m dengan surfaktan. Berikutan ujian regangan kitaran manual, keputusan menunjukkan bahawa rintangan meningkat apabila bilangan kitaran meningkat disebabkan oleh pembentukan retak. Bacaan sifar rintangan pukal 5 μ m dan 15 μ m zarah saiz diperolehi apabila regangan mencapai kira-kira 13 cm hingga 14 cm panjang, iaitu 225% hingga 250% daripada peratusan terikan. Pemanjangan yang dibenarkan bagi kedua-dua saiz zarah untuk bertahan lebih lama dengan rintangan yang lebih baik adalah 125% dengan pemanjangan 0.5 cm dari panjang awal 4.0 cm. Selain itu, didapati bahawa kekuatan lekatan 15 μ m GNP iaitu 0.00419 N/mm adalah lebih baik berbanding 5 μ m GNP iaitu 0.00328 N/mm. Morfologi permukaan setiap zarah digambarkan sebagai hasil daripada rintangan pukal selepas diregangkan melalui kitaran.

اونيورسيتي تيكنيكل مليسيا ملاك

UNIVERSITI TEKNIKAL MALAYSIA MELAKA

ACKNOWLEDGEMENT

Alhamdulillah, all praises to Allah for His blessing for me to complete this Projek Sarjana Muda (PSM) 2. First and foremost, I would like to express my sincere appreciation and sincere gratitude to my supervisor, Dr. Nadlene Binti Razali for essential supervision, support, and encouragement towards the completion of this experimental and report writing.

I would also like to express my deepest gratitude to postgraduate students in Advance Materials Characteristic Laboratory (AMCHAL), Andee Faeldza Bin Dziaudin and the other members in AMCHAL LAB for their assistance, time spent and effort in lab and work analysis. My sincere appreciation also extends to all AMCHAL's staff for their support and invaluable experience and memorable research atmosphere during my last year.

My sincere gratitude to my parents and my friends for their unconditional love, continuous support, encouragement and prayers throughout this study. Lastly, thank you to everyone who had been to the crucial parts of the realization part of this project directly or indirectly. Thank you.

TABLE OF CONTENTS

| | |
|--|------|
| DECLARATION | ii |
| APPROVAL | iii |
| DEDICATION | iv |
| ABSTRACT | v |
| ABSTRAK | vi |
| ACKNOWLEDGEMENT | vii |
| TABLE OF CONTENTS | viii |
| LIST OF TABLES | x |
| LIST OF FIGURES | xi |
| LIST OF ABBREVIATIONS | xii |
| CHAPTER 1 | 1 |
| INTRODUCTION | 1 |
| 1.1 Background..... | 1 |
| 1.2 Problem Statement..... | 2 |
| 1.3 Objective..... | 3 |
| 1.4 Scope of Project..... | 3 |
| CHAPTER 2 | 4 |
| LITERATURE REVIEW | 4 |
| 2.1 Electronic Packaging | 4 |
| 2.2 Conductive filler | 4 |
| 2.2.1 Metal Based Materials..... | 6 |
| 2.2.1.1 Silver..... | 6 |
| 2.2.1.2 Copper..... | 7 |
| 2.2.2 Carbon Based Material | 7 |
| 2.2.2.1 Carbon Nanotube (CNT) | 7 |
| 2.2.2.2 Graphene..... | 8 |
| 2.3 Polymer Binder | 9 |
| 2.3.1 Epoxy Resin | 10 |
| 2.3.2 PEDOT: PSS | 10 |
| 2.4 Factor Affecting Mechanical and Electrical Properties..... | 11 |
| 2.5 Method To Measures Mechanical Properties | 12 |
| 2.5.1 Stretching Test..... | 12 |
| 2.5.2 Torsion Test..... | 13 |

| | | |
|-------------------------------|---|-----------|
| 2.5.3 | Bending Test..... | 14 |
| CHAPTER 3 | | 15 |
| METHODOLOGY | | 15 |
| 3.1 | Introduction..... | 15 |
| 3.2 | Materials | 16 |
| 3.2.1 | Graphene Nanoplatelets | 16 |
| 3.2.2 | Polymer Binder | 17 |
| 3.2.3 | Surfactant..... | 18 |
| 3.2.3.1 | Dimethyl Sulfoxide (DMSO)..... | 18 |
| 3.2.3.2 | Triton X-100 | 19 |
| 3.2.3.3 | Mono Ethylene Glycol..... | 20 |
| 3.2.4 | Solvent..... | 21 |
| 3.2.4 | Substrate | 22 |
| 3.2.5 | Formulation Of Stretchable Conductive Ink | 23 |
| 3.3 | Mixing Process | 24 |
| 3.4 | Printing Process | 25 |
| 3.5 | Curing Process | 26 |
| 3.6 | Characterization Method..... | 27 |
| 3.6.1 | Manual Cyclic Stretch Test Method..... | 27 |
| 3.6.2 | Peel Test Method..... | 29 |
| 3.6.3 | Digital Microscope | 32 |
| CHAPTER 4 | | 33 |
| RESULTS AND DISCUSSION | | 33 |
| 4.1 | Overview..... | 33 |
| 4.2 | The GNP Inks with Fixed Mixing Parameter | 33 |
| 4.2 | Manual Cyclic Stretch Test Analysis..... | 34 |
| 4.2.2 | Surface Morphology of SCI After Manual Cyclic Stretch Test..... | 40 |
| 4.3 | Peel Test Analysis..... | 41 |
| CHAPTER 5 | | 43 |
| CONCLUSION AND RECOMMENDATION | | 43 |
| 5.1 | Conclusion | 43 |
| 5.2 | Recommendation For Further Works | 44 |
| REFERENCES | | 45 |

LIST OF TABLES

| | |
|---|----|
| Table 2.1: The Conductivity of Metal and Carbon Fillers (Huang et al., 2019)..... | 5 |
| Table 2.2: Classified of Metal Based and Carbon Based..... | 5 |
| Table 3.1: PEDOT:PSS Surfactant (Seekaew et al., 2014)..... | 23 |
| Table 3.2: Hybrid Graphene- PEDOT: PSS Formulation For Different Filler And Polymer Loading..... | 24 |
| Table 3.3: Mixing Parameter..... | 24 |
| Table 3.4: Curing Parameter | 26 |
| Table 4.1: The Location Point of Bulk Resistivity | 34 |
| Table 4.2: The Maximum Strain of Bulk Resistivity Using 5 μ m GNP..... | 35 |
| Table 4.3: The Maximum Strain of Bulk Resistivity Using 15 μ m GNP..... | 36 |
| Table 4.4: Bulk Resistivity of SCI Using 5 μ m GNP..... | 38 |
| Table 4.5: Bulk Resistivity of SCI Using 15 μ m GNP..... | 38 |



LIST OF FIGURES

| | |
|--|----|
| Figure 3.1: Flow Chart of General Methodology | 15 |
| Figure 3.2: Graphene Nanoplatelets (GNP) of 5 μ m and 15 μ m | 16 |
| Figure 3.3: Poly(3,4-ethelenedioxythiophene):poly(stylenesulfonate)..... | 17 |
| Figure 3.4: Dimethyl sulfoxide (DMSO) | 18 |
| Figure 3.5: Triton X-100 (TX) | 19 |
| Figure 3.6: Mono Ethylene Glycol | 20 |
| Figure 3.7: Acetone | 21 |
| Figure 3.8: Dimension of TPU substrate..... | 22 |
| Figure 3.9: Beam balance..... | 23 |
| Figure 3.10: Thinky Mixer | 24 |
| Figure 3.11: Manual Screen Printing Process | 25 |
| Figure 3.12: The Memmert Oven..... | 26 |
| Figure 3.13: Manual Cyclic Stretch Test Setup | 27 |
| Figure 3.14: The Region Points of Bulk Resistivity | 28 |
| Figure 3.15: Peel Test Machines..... | 30 |
| Figure 3.16: The Peel Test Sample | 30 |
| Figure 3.17: Epoxy..... | 31 |
| Figure 3.18: Glass Slide Specimen Preparation..... | 31 |
| Figure 3.19: Digital Microscope | 32 |
| Figure 4.1: The GNP Inks of SCI | 33 |
| Figure 4.2: The Region Points of Bulk Resistivity | 34 |
| Figure 4.3: The Illustration of Fine Crack Starting to Appears | 37 |
| Figure 4.4: Graph of Bulk Resistivity against Number of Cycles | 39 |
| Figure 4.5: Coarse Grains of 5 μ m GNP..... | 40 |
| Figure 4.6: Fine Grains of 15 μ m GNP..... | 40 |
| Figure 4.7: Coarse Grains at 10 Cycles Using 5 μ m GNP..... | 41 |
| Figure 4.8: Fine Grains at 10 Cycles Using 15 μ m GNP..... | 41 |
| Figure 4.9: TPU Graph of 5 μ m GNP | 42 |
| Figure 4.10: TPU Graph of 15 μ m GNP..... | 42 |

LIST OF ABBREVIATIONS

| | |
|-----------|--|
| PCB | Printed Circuit Board |
| FPCB | Flexible Printed Circuit Board |
| SCI | Stretchable Conductive Ink |
| CNT | Carbon Nanotube |
| CF | Carbon Fibre |
| CB | Carbon Black |
| SWCNT | Single-Wall Nanotubes |
| MWNT | Multi-Walled Carbon Nanotube |
| PFC | Printed Flexible Circuits |
| PET | Polyethene Terephthalate |
| TPU | Thermoplastic Polyurethane |
| GNP | Graphene Nanoplatelets |
| PEDOT:PSS | poly(3,4-ethylenedioxythiophene) polystyrene sulfonate |
| EG | Mono Ethylene Glycol |
| DMSO | Dimethyl sulfoxide |
| TX | Triton X-100 |

CHAPTER 1

INTRODUCTION

1.1 Background

Recently, the stretchable conductivity ink of electronic applications has gained significant attention from electronic industries. However, a conventional printed circuit board (PCB) has reached its limitation due to a rigid structure applied at a flexible texture. Therefore, the researcher actively explores the replacement. It might be flexible printed circuit boards (FPCB) made of polymer materials resistant to corrosion, moisture, lubricants, temperature, and impact.

At present, customers will purchase a limited range of stretchable electronics products in the market. Their prices remain incredibly high but not fully stretchable and have a standard hard module. Furthermore, these devices have a few issues on water resistance and product costing. However, FPCB technology provided designers with unprecedented levels of flexibility, but it is still a plastic foil that can only adhere to basic surface topographies and reaches its limitations when stretched. (Vieroth et al., 2009)

In this project, stretchable conductive ink is developed subjected to different particle size. The samples will then undergo a stretch test to assess the behaviour of the mechanical, physical, and electrical properties of SCI. A great achievement from these initiatives has the ability to alter our perception of electronics, transforming it from rigid, planar chips to flexible, curvilinear sheets. (Rogers et al., 2010).

1.2 Problem Statement

Conductive inks are composed of conductive fillers, binders, and solvents that give electrical conductivity. The inks are produced with a specially formulated rheology to provide the best performance for a specific printing process. Conductive ink is a versatile material that may be used in various applications, including printed and flexible electronics. Therefore, they may be used to manufacture low-cost and high-performance electronic devices. Conductive ink's components are non-toxic and environmentally safe.

Stretchable Conductive Ink is important for the development of stretchable electronics. The ink should be capable of being strained to at least 20% of its original length for at least 500 cycles without increasing its resistance by more than 30 times its original value while retaining electrical and mechanical integrity. (Mohammed & Pecht, 2016). This is a good approach for this innovative technology because 20% stretchability can suit many current requirements.

In future, the conventional PCB will face the problem due to the flexibility and stretchability of their rigid components. Thus, the SCI development is a great replacement as the alternative way to overcome their flexibility and stretchability. However, to achieve the better performance of SCI, a few problems are still discovered such as conductivity, hydrophobicity and hardness that may be affected during making it stretchable. In addition, the SCI will undergo a few tests to evaluate its reliability on the mechanical factor to endure the mechanical deformation. The printed screen is used along this experimental to reduce the cost of making SCI in large quantity.

1.3 Objective

1. To evaluate the effect of the stretch test on the mechanical and electrical performance of Graphene nanoplatelets (GNPs) on TPU substrate.
2. To investigate the effect of adhesion properties of Graphene nanoplatelets (GNPs) on the substrates subjected to different particle size

1.4 Scope of Project

This project focused more on the manual stretching test experiment to determine the effect of resistivity of SCI for the maximum strain and the applicable elongation stretch with varying particle GNPs size between 5 μ m and 15 μ m. The surface morphology of both particle sizes is analysed by using the optical microscope before and after undergoing the multiple manual cyclic stretch tests. The peel test is also performed to evaluate the effect of adhesion properties that may be affected the SCI performance.

UNIVERSITI TEKNIKAL MALAYSIA MELAKA

CHAPTER 2

LITERATURE REVIEW

2.1 Electronic Packaging

The semiconductor electronics industries work very hard to improve electronic packaging production and assembly. However, during the early stages of the electronic packaging industry, most connection materials used were made of lead (Pb), which is a highly hazardous substance. (Chew et al., 2014). An electronic packaging refers to an electronic device that protects the electronic and electrical system components from each other and the environment. Thus, the stretchable interconnects enable the overall electronic system to withstand large deformation in order to help improve the performance of printed circuit board. In addition, electronic packaging gives protection to mechanical, chemical or electromagnetic components and interconnections (Li, Y. 2007).

2.2 Conductive filler

Conductive filler is a material used to make conductive ink, which is electrically conductive to SCI. In general, the electrical conductivity of a conductive filler is determined by the type of filler and aspect ratio of the conductive filler materials. Thus, a highly conductive filler is added to the composite matrix to form a three-dimensional network of filler particles throughout the component. This critical state is known as the percolation threshold. (Sandler et al., 2003). Percolation theories

are widely used to describe the transitions from insulator to conductor in a continuous conductive network via a composite which is consisting of a conductive filler and an insulating matrix. It has been demonstrated that increasing the aspect ratio of the conductive filler reduces the value of the percolation threshold. (Untereker et al., 2009). Therefore, to obtain high conductivity, the filler concentration must be equal to or higher than the percolation critical concentration.

There are two types of the metal filler used in SCI which is metal and non-metals based. Non-metals based consist of carbon based and conducting polymer. Both types of non-metal can conduct electricity. However, Carbon-based materials are widely used for SCI due to better electrical and mechanical properties compared to polymer-based materials. Table 2.1 shows the conductivity of metal and carbon fillers. Carbon filler consists of carbon fibre (CF), carbon black (CB) and carbon nanotube (CNT) while metallic filler consist of metal flakes, metal powder, metal nanowire and metal coated fibre.

Table 2.1: The Conductivity of Metal and Carbon Fillers (Huang et al., 2019)

| Filler type | Electrical conductivity (S/cm) | Thermal conductivity (W/mK) | Density (g/cm ³) |
|-------------------|--------------------------------|-----------------------------|------------------------------|
| Aluminium | 3.538×10^5 | 234 | 2.7 |
| Copper | 5.977×10^5 | 386-400 | 8.9 |
| Silver | 6.305×10^5 | 417-427 | 10.53 |
| Nickel | 1.43×10^5 | 88.5 | 8.9 |
| CNTs | 3.8×10^5 | 2000-6000 | 2.1 |
| CF | 10^2-10^5 | 10-1000 | 1.5-2.0 |
| Graphene | 6000 | 4000-7000 | 1.06 |
| Graphite | 10^4 | 100-500 | 2.25 |
| Aluminium nitride | $<10^{-13}$ | 100-319 | 3.235 |
| Boron nitride | 10^{-14} | 185-400 | 2.27 |

Table 2.2: Classified of Metal Based and Carbon Based

| Based Material | Metal | Carbon |
|----------------|-------------------------------|------------------------------|
| Filler Type | Silver Aluminium Copper | Graphene CNTs Graphite |

2.2.1 Metal Based Materials

Conductive ink that made up of metal-based material known as metal fillers. Commonly, the fillers are combined together with polymer binders, and solvents, which typically include volatile solvents and non-volatile organic polymers. Conductive fillers that offer conductivity and polymer binders give physical and mechanical properties for conductive ink such as adhesion, stretchability, and influence strength.

2.2.1.1 Silver

Silver-based conductive ink is a metal filler that is commonly used in printed electronic applications to generate a conductive electronic line. Silver is considered a potential replacement of conductive filler due to its strong electrical ($6.3 \times 10^7 \text{ S m}^{-1}$) and thermal conductivity ($429 \text{ W m}^{-1} \text{ K}^{-1}$). (Gao et al., 2011). Besides from excellent charge transport properties, conductive ink for ink-jet and printing applications must also meet general ink requirements such as high conductivity, low resistivity, low viscosity, high chemical stability, low temperature process ability, and surface tension.(D. Y. Wang et al., 2015). Furthermore, the electrical and mechanical properties of silver particles ink are highly dependent on their size, shape, and chemical treatment. Silver nanoparticles with spherical, cubic, and flake-like morphologies exhibit unique characteristics. In comparison to silver nanoparticles with a spherical form, provides greater advantages such as a bigger contact area and superior electrical properties.(Sun et al., 2003)

2.2.1.2 Copper

Copper is a reddish element that has a shiny metallic. It also ductile and malleable materials. Copper base alloys with high electrical or thermal conductivity have gained popularity in a wide variety of electrical applications. In term of thermal conductivity, copper has good thermal conductivity as high of $\lambda=380W/m.K$. However, it has poor mechanical properties which the tensile strength is below 225MPa. (Coddet et al., 2016). Besides, copper has its disadvantages due to instability against oxidation under ambient temperature and it tends to form an insulating layer of copper oxide. Furthermore, the formation of copper oxidation generates poor conductivity in sintered copper films and interferes with the sintering of copper particles. (Coddet et al., 2016).

2.2.2 Carbon Based Material

Carbon-based conductive inks have acquired significant appeal in printed and electronic packaging applications during the last few years due to their low cost, environmental compliance, and lower assembly temperature. The carbon-based materials include carbon black (CB), carbon fibres (CF), graphite, carbon nanotubes (CNTs), and graphene.

2.2.2.1 Carbon Nanotube (CNT)

Carbon nanotube (CNT) is a nano particle conductive filler material with excellent electrical conductivity, lightweight, high strength modulus, and free oxidation. CNTs have a basic structure that can be referred to as single-wall nanotubes (SWCNT) with a single layer rolled tube. Besides, another form of common CNT is multi-walled nanotube (MWCNT), which is rolled into a multi-layer tube. SWCNT

has better electrical properties than MWCNT. Due to its excellent electrical properties, it is suited for use as connecting materials, which have formed the basis for producing modern electronics. (Ayatollahi et al., 2011) Stretchable conductors like CNT were embedded within elastomers making them stretchable. A Carbon Nano Tube CNT tube on polyurethane can handle up to 400% strain (Lee et al., 2012).

2.2.2.2 Graphene

Graphene is a hexagonal crystalline single layer of graphite. Graphene exists in various forms such as graphene nanoplatelets, nano-sheets and 3D graphene. Among these, graphene nanoplatelets are widely used in electronics applications due to their pure graphitic composition which is excellent in electrical and thermal conductors. Graphene nanoplatelets come in black or grey powder.

Graphene inks recently have dramatically improved flexible print electronics since they are cheap, easy to manufacture, more flexible and have a greater conductivity. Graphene is essentially a single atomic layer of graphite, a common material that is an allotrope of carbon composed of extremely closely linked carbon atoms organised in a hexagonal lattice. Graphene is so special in its sp² hybridisation and very thin atomic thickness of 0.345nm. (Mevold et al., 2015). This allowed graphene to surpass so many records for strength, electricity, and heat conduction.

2.3 Polymer Binder

The polymer binder phase is essential for the stretchability of the stretchable conductive inks. In general, the polymer binder in SCI serves to give strong adhesive strength between conductive ink and substrates while also providing stretchability in the sintered form.(Hsu et al., 2013). Furthermore, the adhesive connection must be able to resist the device's whole operational temperature range due to exposed environmental factors during operation.(Hsu et al., 2013).

Thermosetting and thermoplastic resins were frequently utilised as matrix in polymer conductive composites. Polypropylene (PP), polyethylene (PE), and polystyrene are examples of thermoplastic resins (PS). Polypropylene is widely available due to its superior mechanical qualities, great resistance to heat, low cost, ease of processing, and fully recyclability, meanwhile thermosetting resins include epoxy resin, vinyl-ester, and polyester. (Alemour et al., 2018).

Both thermosetting plastics and thermoplastics react differently when heated. Thermoplastics can melt when exposed to heat after curing, whereas thermoset plastics retain their shape and remain solid when exposed to heat once cured. (AlMaadeed et al., 2020). Thermoplastic and thermosetting resins are electrically insulating, with very low electrical conductivity values. (Alemour et al., 2018).

2.3.1 Epoxy Resin

Epoxy that acts as a binder consists of two parts: resin and hardener mixed to cause it to cure. Epoxy resin is the most suitable polymer binder for conductive inks due to its viscosity properties. It is commonly used in demanding applications because of its strong chemical and corrosion resistance, good adhesive qualities, low shrinkage, and inexpensive cost. (Chatterjee et al., 2012)

In this study, the Araldite 506 Epoxy Resin (Bisphenol A-epichlorohydrin) has a density of 1.168g/ml and a viscosity at 500-750 mPa.s 25°C was used as a polymer binder. Epoxy resin is manually mixed up with the Hardener JeffAmine D-230 with 63.75% and 21.25 %, respectively for about 1 minute. A hardener is a solvent applied to the ink mixture to cause it to harden and provide a more durable ink and a curing agent for epoxy. The hardener has a vital role in epoxy water absorption. (Wu et al., 2006).

2.3.2 PEDOT: PSS

PEDOT: PSS is an advanced conducting polymer with high conductivity, excellent electrochemical properties, and low redox potential. Although this polymer is fully organic and non-metal, it could conduct electricity very well. In addition, the other advantage of PEDOT: PSS is used in a wide variety of electronic applications because of its water dispersibility, excellent visible-light transparency, high stability in ambient temperature, mechanical flexibility, and good solubility. (Netnapa et al., 2017). However, Netnapa also states that the more layer of conductive ink, the lower sheet resistivity. The composite contains 1.6 wt.% PEDOT: PSS has a high stretchability of up to 340% but an extremely poor conductivity. (Yang et al., 2020).

When PEDOT: PSS is mixed with filler such as graphene or CNT, it could optimise the electrical, mechanical, thermoelectric and other properties. (Yang et al., 2020)

2.4 Factor Affecting Mechanical and Electrical Properties

Some of the most important factors that can affect the sheet resistance of conductive ink are the curing conditions of the ink, the viscosity of the ink, and the filler content of the ink. (S Merilampi & Ruuskanen, 2009). The other filler properties, such as particle size, might affect the electrical conductivity. It has been demonstrated that smaller particle sizes reduce the percolation threshold for spherical particles. (Zaremba & Smoleński, 2000). Besides, it has been proven that having a greater aspect ratio (length to diameter ratio) and a wider range of aspect ratios reduces the percolation threshold. (Zaremba & Smoleński, 2000). Electrical properties are affected by the composition and amount of polymer matrix, as well as the particles (size, amount, shape, distribution, and orientation).

In addition, the surface properties of the filler and polymer also have a significant effect on the composite's conductivity and percolation threshold. Both the filler and the matrix have free surface energies, and the difference between their surface energies determines how well a polymer wets a filler surface. The polymer wets the filler better when the surface energies are closer together. (E. P. Mamunya, 1997). Therefore, improving the filler's wetting can improve its dispersion inside the matrix material. Thus, the composite's percolation threshold may increase, improving the composite's overall conductivity. For better electrical conductivity, a lower surface energy difference between the filler and the polymer is preferable.

2.5 Method To Measures Mechanical Properties

2.5.1 Stretching Test

The stretch test is performed on a substrate such as TPU and PET to evaluate the electrical performance of stretchable conductive ink for every 1000 cyclic to 5000 cyclic until it is fatigue. It is important to determine the flexibility of the substrate with the filler after a few cyclic tests. (Anwar A. Mohammed, 2017) states during the cycle stretch test. The strain is raised at a constant rate until the conductor fails and no electrical reading is obtained or the resistance beyond a certain limit. The cyclical reliability of a stretchable conductor may be measured by performing a large number of stretch cycles and estimating the conductor lifetime under a certain strain. (Mohammed & Pecht, 2016)

At the initial stages, cracking develops perpendicular to the direction of strain during stretching. On PET conductive ink, cracks begin to appear at 40% strain, and the cracks area increases to 50% strain. On TPU, cracking was first noticed at 20% of strain and increased to 50% strain. (Ashikin et al., 2013) In order to obtain higher conductivity, the conductive ink must minimise crack growth during sample stretching. In this scenario, the TPU substrate conductive ink cracks are greater than those on the PET substrate.

2.5.2 Torsion Test

Torsion testing includes twisting a sample along an axis to get information such as torsional shear stress, maximum torque, shear modulus, and breaking angle of a material or the interface between two materials. Typically, a longitudinal sample is put in a torsion tester and one end of the sample is twisted along the long axis until failure, during which the force, or torque in the case of rotation, and displacement, or angular displacement in the case of rotation, are recorded. (Khan, 2019)

Hannila describes in her article about The Effect of Torsional Bending on Reliability and Lifetime of Printed Silver Conductors. During the test, the test samples are twisted clockwise and counterclockwise for 180 seconds at an angular speed of 950/min. The resistance of the printed conductors is measured using a four-point resistance measurement methodology. Resistance measurements are taken at a sampling rate of 1 Hz. (Hannila et al., 2020). Constant current is supplied by the sample while measuring the voltage drop. In this article, a shunt resistor was used to maintain a consistent supply voltage and monitor the current flowing through each conductor. To minimise the effect on the measurement results, shunt resistors have resistance and tolerance values of 1Ω and 1%.

Moreover, samples are clamped at the connection and printed conductor interfaces to eliminate stress at the interface. The resistance of each conductor was then determined using the measured current and constant supply voltage. The measurement data is filtered to identify six consecutive resistance values that are 20% more than the starting resistance at zero (at 0), indicating that the conductor has failed.(Hannila et al., 2020).

In the other articles, Wang found that MXene nanosheets are resistant to dynamic bending over an extended period by providing constant resistance (Q. W.

Wang et al., 2019). After 1000 cycles of bending, a relatively slight increase in resistance occurs from 39 Ω to 61 Ω . These findings demonstrate the multifunctional textile long-term structural and performance stability, indicating potential applications as intelligent clothing for sensor, actuator, energy generator, and EMI shielding. (Q. W. Wang et al., 2019)

2.5.3 Bending Test

The majority of studies on flexible display dependability are focused on the functional effects of substrate bending. Three-point bending and four-point bending are the most often used experiments in industry. Three-point bending is more practical than four-point bending when considering the display's practical applicability. (Chen et al., 2008). During bending, the conductor film experiences tensile stress while the inner surface experiences compressive stress.

Merilampi, describe in his article that the electrical behaviour of the silver ink when subjected to cyclic bending in a various flexible substrate by used screen printed method. The composition of the polymer matrix and micrometre-sized conductive particles affect both the electrical and mechanical characteristics of silver ink conductors. (S Merilampi & Ruuskanen, 2009). They also discovered the necessity of a protective coating in preserving the flexibility of printed silver conductors during bending was emphasised. Cracking is caused by increased resistance of screen-printed silver conductors under mechanical stress and is the partial breakage of the conductive network due to the applied strain. (Sari Merilampi et al., 2011)

CHAPTER 3

METHODOLOGY

3.1 Introduction

This chapter 3 discusses the entire experiment on the technique of preparing the GNPs inks and its processes such as mixing, printing, and curing, as well as the characterization of the manual setup cyclic stretch test and peel test. The flow chart is also included to provide an idea of the whole procedure of this research.

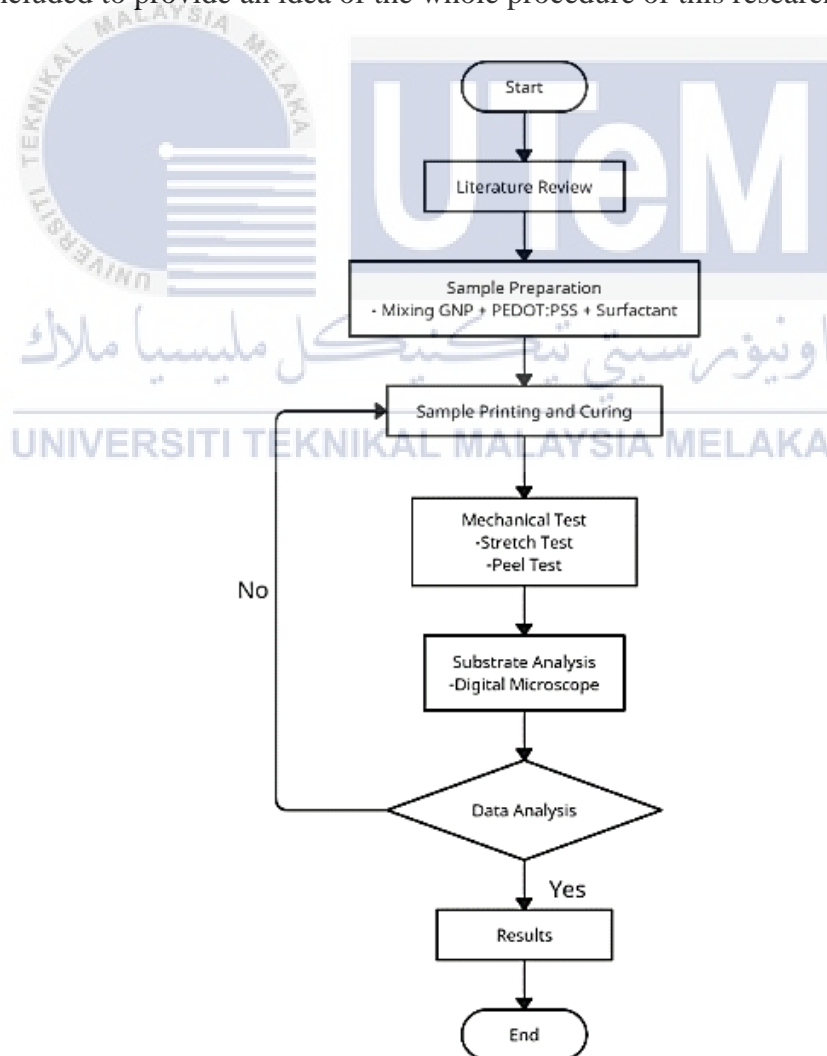


Figure 3.1: Flow Chart of General Methodology

3.2 Materials

3.2.1 Graphene Nanoplatelets



Figure 3.2: Graphene Nanoplatelets (GNP) of 5 μ m and 15 μ m

Graphene nano-platelets (GNP) was used as nano-filler particles to improve the characteristics of polymer composites such as thermal, electrical, and mechanical properties. Composites with enhanced thermal conductivity GNP are utilized in thermal management applications. GNP is considered a good electrical conductor. However, GNP with low filler concentration may not become an electrical conductor but more to high thermal conductivity properties (Hung et al., 2006).

In this experiment, the comparison is made between both particle sizes, 15 μ m and 5 μ m of GNP with 7.5wt% filler loading to evaluate the mechanical and electrical performance. The morphology surface is analysed before and after the manual stretch test and peel test experiment.

3.2.2 Polymer Binder



Figure 3.3: Poly(3,4-ethelenedioxythiophene):poly(stylenesulfonate)
(PEDOT:PSS)

Poly(3,4-ethelenedioxythiophene):poly(stylenesulfonate) (PEDOT:PSS) is utilised as a polymer binder in a wide variety of electronic applications due to its water dispersibility, excellent visible-light transparency, high stability under ambient conditions, mechanical flexibility, and superior solubility. As a result, PEDOT:PSS has been widely used in hybrid systems as both a host and a guest material to improve electrical conductivity and performance. Through surface modification and stabilisation procedures, graphene is an excellent choice for fabricating conductive composites with PEDOT:PSS. Graphene is of great interest as a revolutionary carbon nanomaterial due to its unique electrical and optical properties, good conductivity, high transparency, high bendability, and excellent stability.(Yoo et al., 2014)

3.2.3 Surfactant

3.2.3.1 Dimethyl Sulfoxide (DMSO)

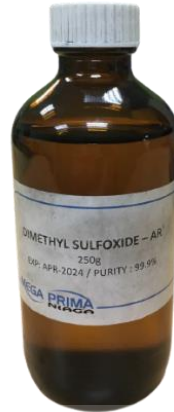


Figure 3.4: Dimethyl sulfoxide (DMSO)

At room temperature, DMSO is the main solvent used to improve the layer's conductivity because it has good conductivity and a low resistance. Thus, by combining DMSO with PEDOT: PSS, conductivity can be increased the sheet resistance of the film, was reduced from 570 to 0.16 k/sqm. However, the DMSO-modified PEDOT:PSS film was not homogenous due to its high viscosity. The contact angle decreased from 49.5° to 31.2° , because the ink was slightly diluted (Liu et al., 2021).

DMSO is used to make PEDOT:PSS formulations more conductive because it can dissolve the PSS shells and make connections among conductive PEDOT grains. In addition surfactant of DMSO further adjust the surface tension and wetting capability of the ink; in fact, owing to their amphiphilic nature, they can easily migrate to any type of surface.(Cinquino et al., 2021)

3.3.3.2 Triton X-100



Figure 3.5: Triton X-100 (TX)

Triton X-100 can be used to enhance the spreadability of PEDOT:PSS inks and as a stabilising agent. The addition of Triton X-100 enhanced the ink's spreading ability and reduced the contact angle from 31.2° to 17.9° . (Liu et al., 2021). Analysis of the electrical, structural, mechanical, and compositional properties of TX show that it plays a role in PEDOT:PSS when it is mixed with TX.

To improve the electrical conductivity, the nonionic surfactant Triton X-100 was added. This makes the ionic interaction between PEDOT and PSS weaker, causing the phase separation into TX-PEDOT and TX-PSS, which makes the electrical conductivity better. (Yoon & Khang, 2016). Thus, optimising post-annealing parameters like as temperature and duration is necessary to attain high conductivity.

3.3.3.3 Mono Ethylene Glycol



Figure 3.6: Mono Ethylene Glycol

Mono Ethylene Glycol contributes to the viscosity and surface tension of the ink, as well as the prevention of quick drying and clogging of the printer head. Among numerous other uses for concentrated graphite dispersions, this technique has been used to develop graphitic inks for inkjet printing. (Capasso et al., 2015).

The mono ethylene glycol was added to the ink not only as a binder but also to change the physical properties such as viscosity, surface tension, and density. Therefore, the printing quality is determined by the ink's physical properties (density, viscosity, and surface tension), as well as the diameter of the nozzle and the droplet velocity. (Romagnoli et al., 2016). The concept of solubility parameters is not only useful for predicting the solute's solubility in a solvent, but also for improving dispersion and adhesion.

3.2.4 Solvent



Figure 3.7: Acetone

The solvent provides viscosity elements, acts as a carrier for the ink, can be highly soluble in polymeric binder, and exhibits great homogeneity. The viscosity features of ink justify its spreadability, with lower viscosity ink having more spreadability. Most of the time, either passive drying or active drying takes place. The main thing to look for when choosing a solvent is how quickly it evaporates. This determines how long the printed ink should dry.

In order to clean the substrate before the screen printing process, the acetone is gently swept before applying the formulation to the substrate without shrinking the TPU. The other application of acetone is used as the solvent to enhance the graphene for stable dispersions. (Htwe et al., 2021)

This process is related to the adhesive bonding between filler and substrate. The substrate is cleaned up by using acetol before putting the filler on the substrate to ensure the surface is clean and easy to adhere. It is important to control the lower or higher wettability for adhesion.

3.2.4 Substrate

The substrate acts as the printing medium and must be able to withstand the curing temperature. Furthermore, the substrate properties must be maintained constant throughout the experiment to avoid altering the ink during the curing process.

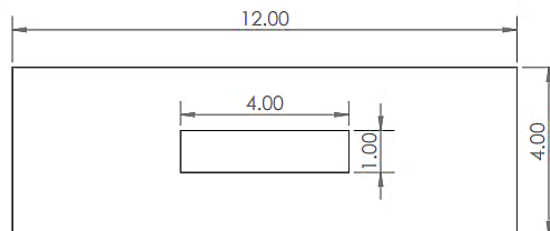


Figure 3.8: Dimension of TPU substrate

The figure 3.8 shows the dimension of the substrate in cm. In this experiment, Thermoplastic polyurethane (TPU) is used as the substrate because it is applicable for undergoing multiple cyclic stretch tests. TPU belong to the polyester polymer group, and they are also known as the most flexible and stretchable substrate explored by numerous researchers.

TPU is a very stretchable substrate. Thus, it was protected with one fine rigid layer to make it firm for the preparation filler to be printed on the substrate. It also helps to minimize uneven surfaces such as wrinkles or bubbles during applying the scotch tape around the GNP to manually print on the substrate. The fine rigid layer will peel off after the curing process was done.

The TPU should be stored in a safe place at room temperature and not overlap with other TPU without a cover after the curing process. The precautions should be taken to ensure that the filler does not crack or touched when opening the scotch tape on the TPU as it will affect the mechanical and electrical performance.

3.2.5 Formulation Of Stretchable Conductive Ink

The first step is to prepare all the materials that need to be weighed using a beam balance apparatus, as illustrated in figure 3.9 below. The polymer binder was utilised with the other solution in order to enhance the optimal performance of SCI. Therefore, the mass for every surfactant was weighed followed the formulation data on Table 3.1



Figure 3.9: Beam balance

Table 3.1: PEDOT:PSS Surfactant (Seekaew et al., 2014)

| PEDOT:PSS solution Mass, g | PEDOT:PSS (wt%) | PEDOT:PSS Mass, g | DMS O (wt%) | DMS O mass, g | EG (wt%) | EG mass, g | Triton x-100 (wt%) | Triton x-100, g |
|----------------------------|-----------------|-------------------|-------------|---------------|----------|------------|--------------------|-----------------|
| 1 | 89.82 | 0.898 | 5.98 | 0.0598 | 3.99 | 0.0399 | 0.199 | 0.199 |

At the first stage, the PEDOT: PSS with a weight concentration of 89.82 wt% and all surfactants will be dissolved together in one container according to the weight concentration percentage in 1 gram as shown in Table 3.1. However, for the triton solvent, it has a very lower significant mass in gram to be controlled when put or drop in the container. For 1 gram of triton mixture solvent, it would be 0.00199g. Thus, one drop of triton will excess a bit and it is acceptable to approximate to 0.00199g in this test experiment.

For the second stage, the other balanced of 10.18 wt% of weight concentration of filler which is GNP is added into the container to mix up again. Both polymer and solvent are mixed up at the first stages then mixed up again with the GNP for the second stages as shown in Table 3.2, to ensure the GNP was mixed well together and could give a better characteristic in terms of its contact angle and resistivity and adhesion reading values.

Table 3.2: Hybrid Graphene- PEDOT: PSS Formulation For Different Filler And Polymer Loading

| Sample | SCI mass, g | Graphene (wt%) | Graphene mass, g | PEDOT: PSS solution (wt%) | PEDOT: PSS Ink Mass, g | Substrates |
|--------|-------------|----------------|------------------|---------------------------|------------------------|------------|
| 1 | 1 | 7.5 | 0.07 | 92.5 | 0.93 | TPU |

3.3 Mixing Process

The Thinky Mixer is used to mix the pedots, solvent and GNP with the desired percentage according to the optimal formulation. Along with this experiment, all the parameter of speed and time to mixer was constant which is 400rpm for 10minutes.

Table 3.3: Mixing Parameter

| | |
|--------------------|-----|
| Mixing Speed (rpm) | 400 |
| Mixing Time (min) | 10 |



Figure 3.10: Thinky Mixer

The mixer parameter will affect the factor of contact angle in this experiment. These factors include the surface energy of the surface, the roughness, the real contact area, and the chemical composition of the ink. Therefore, the measurement of the contact angle, which reflects the degree of wetness when a solid and a liquid interact, is used to research hydrophobicity.

3.4 Printing Process

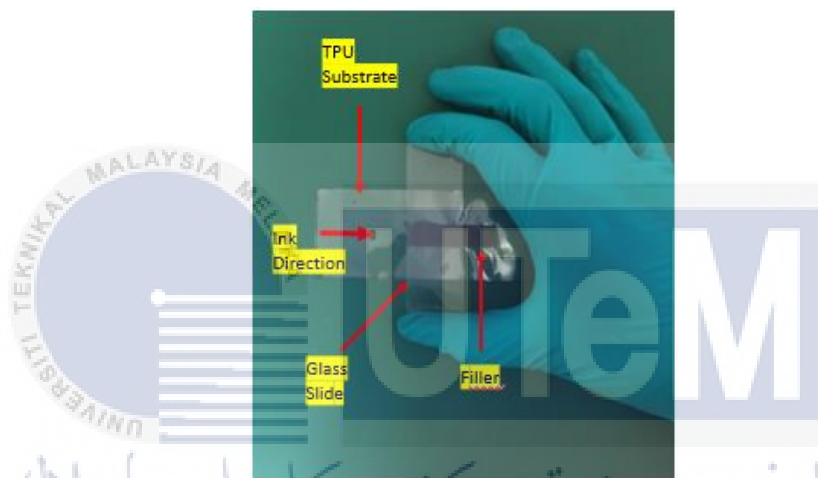


Figure 3.11: Manual Screen Printing Process

Screen printing is a low-cost patterning method for constructing a circuit by applying conductive filler to a stretchable base material. In this experiment, the GNP is manually put at the middle of the substrate and spread uniformly by using the glass slides followed by the rectangular pattern on substrate (4cm x 1cm) size.

The thickness of the filler is manually controlled to ensure the filler spread on all areas. To obtain a good appearance on the substrate, applied two layers which let the first layer dry and applied the second layer to get the best appearance surface.

The main limitation of manual screen printing with GNP inks is the difficulty in determining the thickness of the printed pattern, which is mostly determined by the

stencil thickness. Besides, there is a challenge in creating extremely viscous and concentrated graphene dispersions due to graphene's natural inclination toward aggregation. Furthermore, manual screen printing needs extra skill to ensure the ink is fully spread and does not have any porosity or bubble in order to obtain a good surface appearance for SCI testing.

3.5 Curing Process

The curing process techniques use radiation to manipulate heat in order to evaporate binders and undesired solvents in conductive inks, leaving only hardened metallic material of GNP on the substrate that adheres to the intended substrate. During the curing process, the polymer binders and fillers condense, and the conductive filler provides a pathway for the flow of electric current. An incomplete curing process will lead the polymer to absorb more water and reduce adhesive strength.



Figure 3.12: The Memmert Oven

Table 3.4: Curing Parameter

| | |
|-------------------------|----|
| Curing temperature (°C) | 60 |
| Curing Time (min) | 15 |

In this experiment, the curing process is carried out for 15 minutes at 60°C to ensure the adhesion of GNP ink to their substrate in order to improve the mechanical and electrical properties. The oven is heated first until it maintains 60°C and then, the tray is put inside and moved as close to the oven's filament as possible to ensure that direct heat is applied to the specimens. In general, higher conductivity may be achieved by heating to a higher temperature and burning away any organic contaminants solvents. (Khirotdin et al., 2017).

3.6 Characterization Method

3.6.1 Manual Cyclic Stretch Test Method

A cyclic stretch test is conducted to determine the maximum strain of both particle sizes, 15µm and 5µm. This cyclic stretch test experiment indicated the resistivity reading and surface morphology conditions for every cyclic loading. The strain test was tested until the ink of the sample cracked and did not have any resistance reading which it has reached the maximum point of crack propagation.



Figure 3.13: Manual Cyclic Stretch Test Setup

1. Setup the stretch strain experiment as shown in figure 3.13.
2. The completed sample was placed on the cutting board and a ruler is placed next to the sample of SCI.
3. Fixed the clamp on the left side with the sample on two glass slides to elevate it. Then, clamp the right side of the substrate and make it free to be pull for cyclic stretch.
4. The resistivity was evaluated by using a multimeter for every cyclic cycle until 20 cycles for the elongation
5. The resistance data and surface morphology were recorded for every 5 cycle until 20 cycle of cyclic strain stretch test

The formula to find the maximum strain of stretch test is shown below:

$$\frac{Final - Initial}{Initial} \times 100$$

The resistance reading was varied for every region to indicate the value of resistance. The resistance reading was tested on region 1 and region 2 with different point and repeated with different cyclic stretch loading and the data was recorded to be analyse.

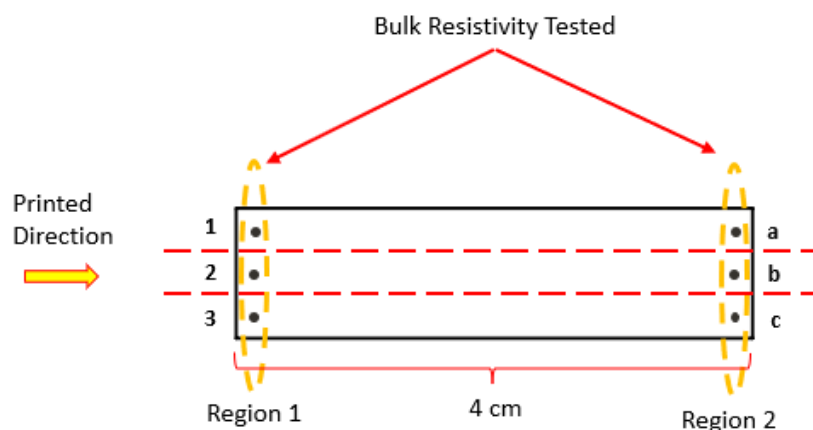


Figure 3.14: The Region Points of Bulk Resistivity

In theory, the longer the distance between the test point of resistance, the higher the resistance value. Meanwhile, the shorter the length, the lower the resistance value. The resistance length tested of sample was fixed and approximately 4cm at both end side of the filler.

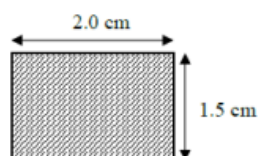
Manual cyclic stretch test was used to determine the maximum strain for both 5 μ m and 15 μ m particle sizes. Both samples were stretched to their maximum strain, which is no longer data indicating resistance. Each condition of the cyclic stretch test is recorded in order to identify the optimal state for the filler prior to cracking. The optimal condition or appearance of the filler before its crack was used to decide the reference length to stretch in the subsequent cyclic stretch experiment.

3.6.2 Peel Test Method

A Peel test is conducted to determine the adhesion strength between GNP ink and the substrate. The filler will be printed on the slight top on the substrate with the dimension of 20 mm x 15 mm. The procedure of the peel test experiment is set up as below.

180° Peel Test.

1. The conductive ink was printed on TPU substrate with the dimension of 20 mm x 15 mm.



2. The printed conductive ink was fixed on the glass slide with epoxy.
3. The adhesion strength was evaluated by using 50 N load cells of a Universal Tensile Machine.

- The glass slide and TPU substrate were attached to the top and bottom grip of the tensile test jigs respectively.

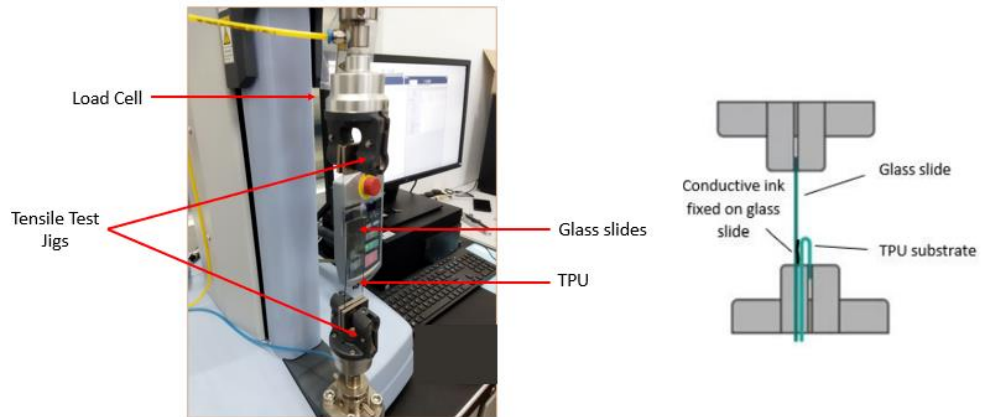


Figure 3.15: Peel Test Machines

- The sample was pulled at speed of 10 mm/min.

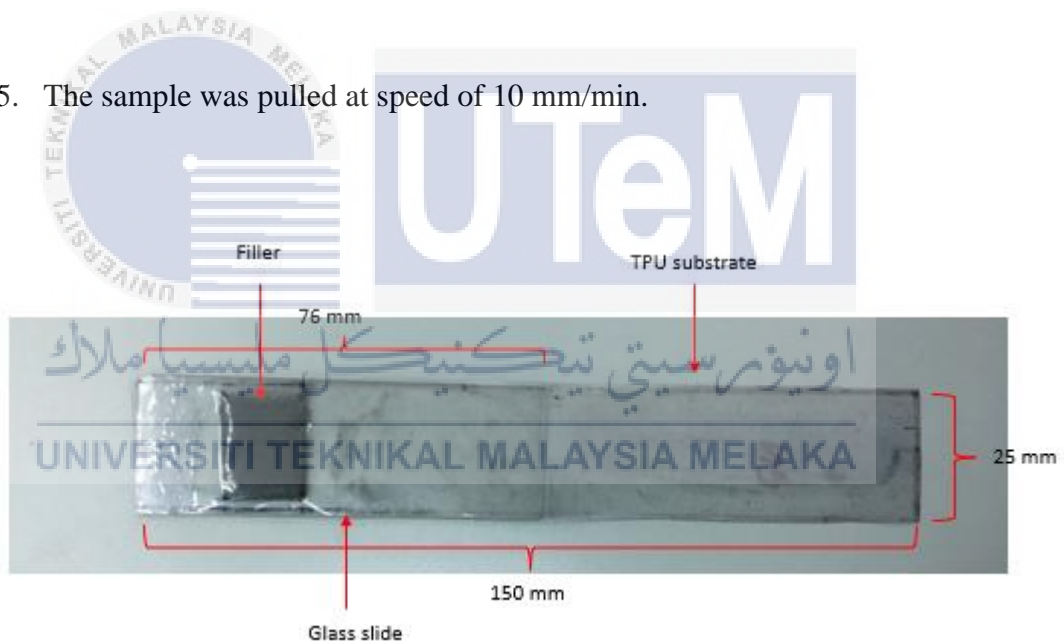


Figure 3.16: The Peel Test Sample

Figure 3.16 shows the ready sample of the peel test to be tested. The dimension of the TPU substrate for the peel test is 25mm x 150mm while the dimension of the glass slide is 25mm x 76mm. Both substrate and glass slides will adhere with epoxy according to the description given of mixing ratio as shown in figure 3.17.



Model Number: DP420
 Brand Name: 3M

substrate: epoxy
 capacity: 50ml
 operating time: 0-20min
 mixing ratio: B/A=2:1

THE OFF-WHITE 3M glue features are as follows:

1. the tough epoxy resin of medium operation time reaches the operation intensity for 1~2hours
2. High performance
3. The approximate value of viscosity is 75 degrees F (24 degrees C) cps: 45000
4. T type stripping (plw) at 75 degrees F (24 degrees C), 5005 verlap shear strength (psi):
 - 1), -67 degrees F (-55 degrees C): 4500
 - 2), 75 degrees F (24 degrees C): 4500
 - 3), 180 degrees F (82 degrees C): 450
 - 4), 250 degrees F (121 degrees C): 200

Figure 3.17: Epoxy

The epoxy needs to apply uniformly on the ink surface contact area only as shown in figure 3.18. As the result of the peel test experiment, the exact data and graphs can be read only on the ink surface area adhered to the glass slide only and not on the surface without ink.

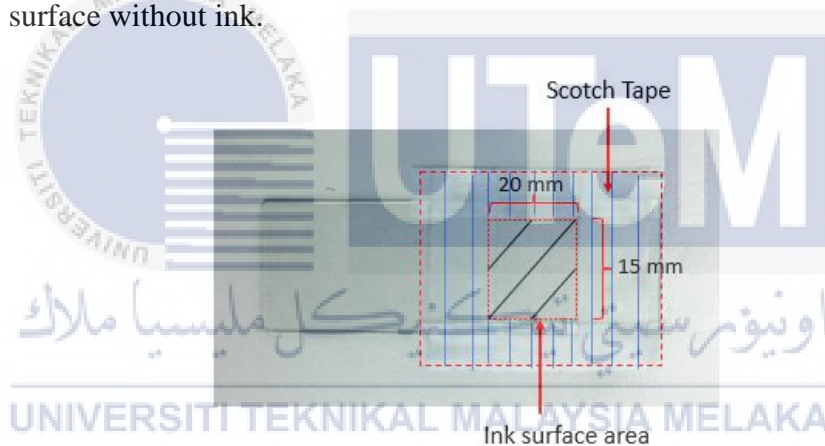


Figure 3.18: Glass Slide Specimen Preparation

To prevent from the excessive epoxy. The scotch tape was prepared to surround the dimensions of 20 mm x 15 mm on the glass slide. Then, gently apply the epoxy to the glass slide on the ink surface area. The excess epoxy was then simply removed by using acetone on the scotch tape and peeling off the scotch tape. After that, properly adhere the sample to the glass slide and allow the epoxy to dry for 1-3 hours before performing the peel test experiment.

3.6.3 Digital Microscope



Figure 3.19: Digital Microscope

The digital microscope examines the surface morphology of GNPs on the substrate to determine the distribution of ink spots. A digital microscope can examine the surface morphology of a sample several times, even if it has been printed with multiple layers of thickness. It can also capture the sample after it has been used several times.

A digital microscope's zooming and illumination system reveal some ink qualities such as specular reflection, gloss, gap, and ink dispersion at point intersections. The digital microscope was positioned perpendicular to the SCI sample sheet and zoomed in on the intersection point. The images were observed and captured directly on the monitor of the computer.

The formation of conductive ink crack can simply be checked by a digital microscope. The behaviour or surface will respond to the value of resistivity when tested using the multimeter. The surface morphology will indicate the formation of crack propagation during the manual cyclic stretch test experiment.

CHAPTER 4

RESULTS AND DISCUSSION

4.1 Overview

Chapter 4 will discuss briefly about the final result of manual cyclic stretch test experiment to determine the effect of resistivity and maximum strain of Stretchable Conductive Ink (SCI) with varying particle size. These chapter will be explained in detail about the resistivity reading that related to the behaviour of SCI surface morphology after multiple cyclic stretch test. The final results of peel test also discussed in this chapter 4 to evaluate the effect of adhesion properties that may be affected the SCI.

4.2 The GNP Inks with Fixed Mixing Parameter



Figure 4.1: The GNP Inks of SCI

GNP particle sizes of $5\mu\text{m}$ and $15\mu\text{m}$ were mixed by using a thinky mixer with a fixed mixing parameter of 400 rpm for 10 minutes. However, the condition of GNP inks differs from each other for both particle sizes. Figure 4.1 shows that $5\mu\text{m}$ GNP have a coarse grain of conductive inks due to clumpy ink while for $15\mu\text{m}$ GNP

obtained a fine grain of conductive inks after the mixing process. Therefore, various GNP particle sizes will give different characteristics in terms of their mechanical and electrical performance results. The coarse grains will provide more electron transport from one grain to another grain, playing a significant role to decrease the resistivity of conductive ink. (Mou et al., 2018)

4.2 Manual Cyclic Stretch Test Analysis

Table 4.1 shows the five location points of bulk resistivity while figure 4.2 shows the region points of bulk resistivity that need to be tested by using the multimeter. The bulk resistivity or resistance was varying for each point. After multiple stretching tests, some points will experience more fatigue due to the extremely compressed and tension forces acting on them. Thus, the resistivity is higher at some point when the cyclic stretch increases. In general, the higher the resistivity, the lower the conductivity of SCI.

Table 4.1: The Location Point of Bulk Resistivity

| Point No. | Point Location |
|-----------|----------------|
| 1. | 1-a |
| 2. | 2-b |
| 3. | 3-c |
| 4. | 1-c |
| 5. | 3-a |

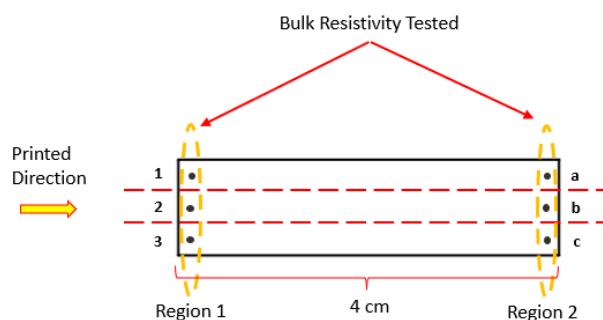


Figure 4.2: The Region Points of Bulk Resistivity

In the first stages, the experiment was started to determine the maximum strain of bulk resistivity for 5 μ m and 15 μ m GNPs particles size. The sample was stretched by using the manual cyclic stretch test jig and the resistivity reading was tested by using the multimeter until it indicated zero values of bulk resistivity. Both GNPs particles size of experimental results is shown in table 4.2 and table 4.3.

Table 4.2 shows the maximum stretch strain of bulk resistivity using 5 μ m GNP. From the observation in data table 4.2, the 5 μ m GNP reaches its limit cyclic stretch at 10cm elongation which is 250% of the strain percentage, before one of the test points showed the zero values of bulk resistivity or resistance. The point of resistance was fully zero when it reaches a 13cm cyclic stretch for 5 μ m GNP.

Table 4.2: The Maximum Strain of Bulk Resistivity Using 5 μ m GNP

| Length cm | Strain % | Resistance, Ω | | | | |
|--------------|-------------|----------------------|-------|-------|-------|-------|
| | | 1 | 2 | 3 | 4 | 5 |
| 0 | 0 | 100 | 76 | 126 | 113 | 72.6 |
| 1 | 25 | 239 | 231 | 282 | 275 | 220 |
| 2 | 50 | 472 | 376 | 425 | 498 | 503 |
| 3 | 75 | 0.78k | 0.67k | 0.83k | 0.8k | 0.90k |
| 4 | 100 | 2.4k | 1.63k | 1.78k | 2.94k | 1.5k |
| 5 | 125 | 2.67k | 2.20k | 2.70k | 3.79k | 2.3k |
| 6 | 150 | 5.3k | 5.2k | 4.33k | 5.97k | 4.9k |
| 7 | 175 | 6.61k | 6.7k | 7.35k | 9.2k | 6.70k |
| 8 | 200 | 7.05k | 7.6k | 8.55k | 11.6k | 7.9k |
| 9 | 225 | 8.7k | 9.9k | 9.87k | 13.3k | 9.3k |
| 10 | 250 | 13.0k | 12.4k | 11.4k | 15.3k | 13.7k |
| 11 | 275 | 14.3k | 0 | 0 | 17.8k | 15.4k |
| 12 | 300 | 16.7k | 0 | 0 | 0 | 19.4k |
| 13 | 325 | 0 | 0 | 0 | 0 | 0 |

Table 4.3 shows the maximum stretch strain of bulk resistivity using 15 μ m GNP. From the observation in data table 4.3, the 15 μ m GNP reaches its limit cyclic stretch at 10cm which is 250% of the strain percentage, before one of the test points showed the zero values of bulk resistivity or resistance. The point of resistance was fully zero when it reaches a 12cm cyclic stretch for 15 μ m GNP.

Table 4.3: The Maximum Strain of Bulk Resistivity Using 15 μ m GNP

| Length cm | Strain % | Resistance, Ω | | | | |
|--------------|-------------|----------------------|-------|-------|-------|-------|
| | | 1 | 2 | 3 | 4 | 5 |
| 0 | 0 | 38.5 | 40.2 | 45.5 | 34.6 | 46.2 |
| 1 | 25 | 112.3 | 114.3 | 132.5 | 91.3 | 124.5 |
| 2 | 50 | 178.5 | 258.1 | 264.7 | 221.3 | 239.4 |
| 3 | 75 | 476.3 | 465.3 | 464.3 | 340.1 | 362.3 |
| 4 | 100 | 743.5 | 904.2 | 2.76k | 745.6 | 784.1 |
| 5 | 125 | 1.68k | 3.73k | 3.8k | 946.2 | 2.1k |
| 6 | 150 | 3.7k | 5.1k | 6.8k | 5.5k | 4.3k |
| 7 | 175 | 8.7k | 7.3k | 9.7k | 8.4k | 7.9k |
| 8 | 200 | 14.3k | 13.2k | 14.5k | 13.4k | 10.8k |
| 9 | 225 | 25.9k | 27.7k | 29.3k | 25.4k | 23.5k |
| 10 | 250 | 36.7k | 31.6k | 32.6k | 33.7k | 34.8k |
| 11 | 275 | 49.3k | 0 | 0 | 0 | 0 |
| 12 | 300 | 0 | 0 | 0 | 0 | 0 |

The comparison between 5 μ m and 15 μ m of GNPs particle size can be seen through both data tables of the initial and final value of resistance or bulk resistivity. table 4.2 shows the higher value of resistance for 5 μ m GNP at the initial reading compared to the 15 μ m GNP in table 4.3. However, the final reading in table 4.2 shows the 15 μ m could stretch longer with the higher bulk resistivity compared to 5 μ m in

table 4.2 before it obtained a zero resistivity value. Both particle sizes reveal the starting zero-reading of bulk resistivity occurred at the middle point, which represents the higher stress concentration. As a result, that centre point has achieved its maximum stretch before the rest of the points fatigue.

In the second stage, figure 4.3 shows the illustration of a fine crack starting to appear when it was continued stretched. The crack that appears at the length of 4.5 cm was used as the reference for every cyclic stretch test. This is because, whereas the optimal length to stretch is applicable to withstand longer with better bulk resistivity. The experiment was repeated for 5, 10, 15, and 20 cycles for 5µm and 15µm particle sizes. In general, all of the readings show a rise in the resistance value when stretching. The changes in surface morphology are investigated for every fifth cyclic stretch test. The initial length was fixed at 4.0 cm throughout the experiment.

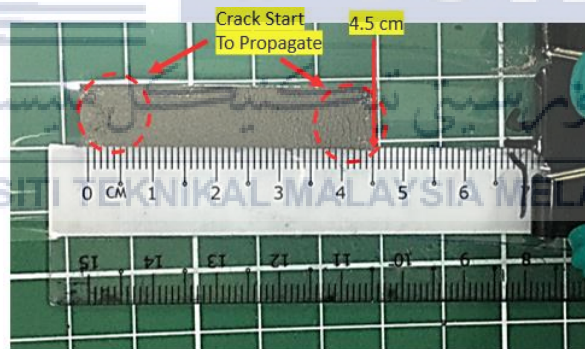


Figure 4.3: The Illustration of Fine Crack Starting to Appears

The formula to find the percentage of strain is shown below:

Initial length = 4.0cm

Final length = 4.5cm

$$\frac{Final - Initial}{Initial} \times 100$$

$$\frac{4.5 - 4.0}{4.0} \times 100 = 125\%$$

Therefore, the optimal strain percentage for both particle sizes that is applicable to withstand longer with better bulk resistivity is 125% with an elongation of 0.5 cm from the initial length of 4.0 cm. The TPU substrate also reaches its limit when it was stretched more than 15cm so the TPU substrate was not applicable to stretch anymore after that point.

Table 4.4 and Table 4.5 shows the data of bulk resistivity of the 5 μ m and 15 μ m GNP respectively. Both samples will perform manual cyclic stretch test cycles which is need to be stretched until 4.5cm according to optimal stretch length to withstand longer with better bulk resistivity. Every 5, 10, 15 and 20 cycles need to be analysed before and after the experimental under the optical microscope to check the condition of surface morphology of both GNPs sample sizes.

Table 4.4: Bulk Resistivity of SCI Using 5 μ m GNP

| Cycles | Length (cm) | Strain % | Resistance, Ω | | | | | Averages |
|--------|-------------|----------|----------------------|-------|-------|-------|-------|----------|
| | | | 1 | 2 | 3 | 4 | 5 | |
| 0 | 4.0 | 0 | 52.7 | 41.7 | 48.1 | 41.6 | 48.2 | 46.46 |
| 5 | 4.5 | 12.5 | 110.3 | 91.6 | 97.6 | 92.4 | 97.8 | 97.94 |
| 10 | 4.5 | 12.5 | 139.9 | 115.2 | 117.3 | 120.7 | 136.6 | 129.94 |
| 15 | 4.5 | 12.5 | 193.2 | 158.3 | 214.3 | 196.5 | 176.4 | 171.74 |
| 20 | 4.5 | 12.5 | 226.5 | 210.5 | 223.5 | 224.5 | 219.3 | 220.86 |

Table 4.5: Bulk Resistivity of SCI Using 15 μ m GNP

| Cycles | Length (cm) | Strain % | Resistance, Ω | | | | | Averages |
|--------|-------------|----------|----------------------|------|------|------|------|----------|
| | | | 1 | 2 | 3 | 4 | 5 | |
| 0 | 4.0 | 0 | 17.5 | 16.4 | 17.1 | 19.2 | 17.6 | 16.96 |
| 5 | 4.5 | 12.5 | 39.1 | 37.7 | 37.1 | 38.6 | 37.5 | 37.4 |
| 10 | 4.5 | 12.5 | 49.3 | 45.4 | 43.2 | 49.2 | 44.3 | 45.68 |
| 15 | 4.5 | 12.5 | 57.6 | 52.4 | 53.6 | 54.3 | 58.1 | 55.2 |
| 20 | 4.5 | 12.5 | 77.2 | 69.3 | 70.1 | 70.6 | 71.2 | 71.08 |

Figure 4.4 shows the graph comparison between 5 μ m and 15 μ m GNPs particle sizes of bulk resistivity. From the observation, the particle sizes of 5 μ m GNP have a higher bulk resistivity compared to the 15 μ m GNP when the number of cycles is increased. This is because the 5 μ m GNP particle sizes obtained the clumpy inks after the mixing process cause the coarse grain problem. This condition happened due to an imperfect mixing process parameter which is not suitable for 5 μ m. The ink dispersion is not fully mixed or evenly distributed. Other factors that may have affected the higher bulk resistivity include the filler being too thick in some areas or uneven surfaces.

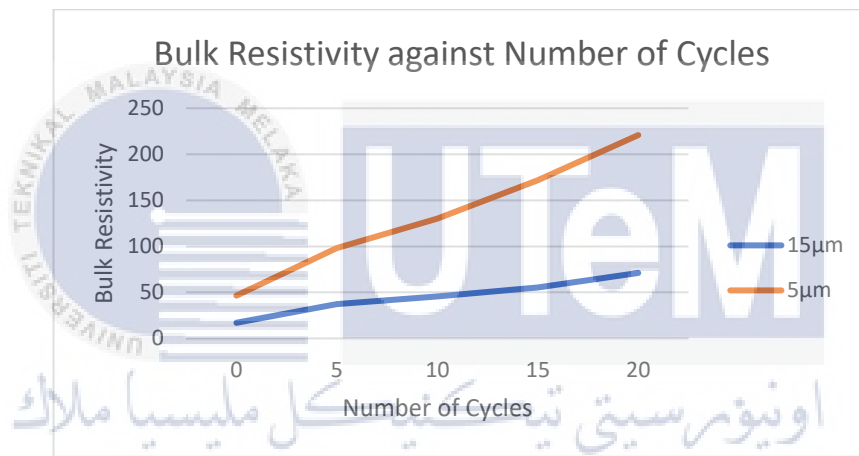


Figure 4.4: Graph of Bulk Resistivity against Number of Cycles

Figure 4.5 and figure 4.6 show the initial surface morphology of both particles sizes of 5 μ m and 15 μ m under the digital microscope. The initial bulk resistivity is represented at 0 cycles in tables 4.4 and table 4.5. The correlation between the surface morphology and resistivity play a crucial role in order to obtain the optimum electrical and mechanical performance. The particle sizes of 5 μ m GNP whereas the coarse grains will result in the higher bulk resistivity, while particle sizes of 15 μ m GNP which has a fine grain, which will result in the lower bulk resistivity at initial conditions compared to 5 μ m.



Figure 4.5: Coarse Grains of 5µm GNP



Figure 4.6: Fine Grains of 15µm GNP

4.2.2 Surface Morphology of SCI After Manual Cyclic Stretch Test

During an experiment, certain samples failed to stretch due to uncontrolled thickness of filler or uneven surfaces conditions. The second failure happened because of the technique or method used to stretch the TPU substrate. When the forces acting on both sides are unbalanced during stretching, some of the regions could shatter or crack, resulting in inconsistency in the resistivity data.

Figure 4.7 and 4.8 shows the surface morphology for both GNP particle size of 5µm and 15µm. The surface morphology was determined by using a digital microscope on the sample's surface. Both particles' sizes show the crack begins to propagate at 10 cycles and continues until 20 cycles. Therefore, both particle sizes could withstand the cyclic stretch test for at least 10 cycles before cracking.

The surface morphology indicated that 5µm GNP has the more significant surface changes at 10 cycles compared to 15µm GNP. This is because 5µm GNP has

a higher coarse grain due to the mixing process not mixing well and the dispersion of filler not being evenly distributed, so that some regions of filler are easily cracked when continuously subjected to the manual cyclic stretch test. Thus, the resistance reading was increased when the cycle increased.

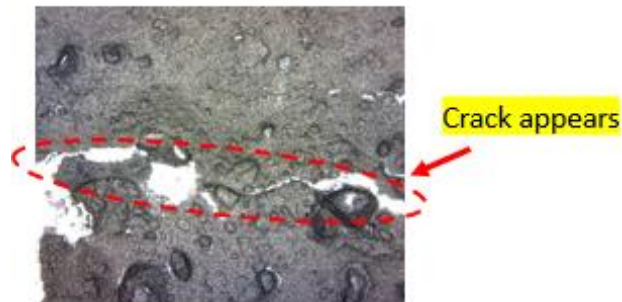


Figure 4.7: Coarse Grains at 10 Cycles Using 5µm GNP

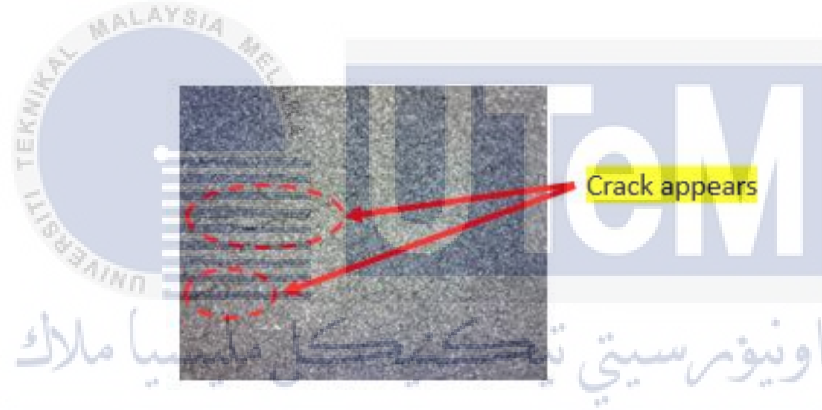


Figure 4.8: Fine Grains at 10 Cycles Using 15µm GNP

4.3 Peel Test Analysis

Peeling force is a crucial parameter for determining the adherence of SCI. This force is defined as the amount of force necessary to separate an adhesive ink from a substrate. Peel strength is a parameter that indicates the average force required to separate two bonded between filler and TPU substrate. The strength is computed by multiplying the unit width of the bonded samples by the average force (the peel force) required during the test. The test is done for 180°.

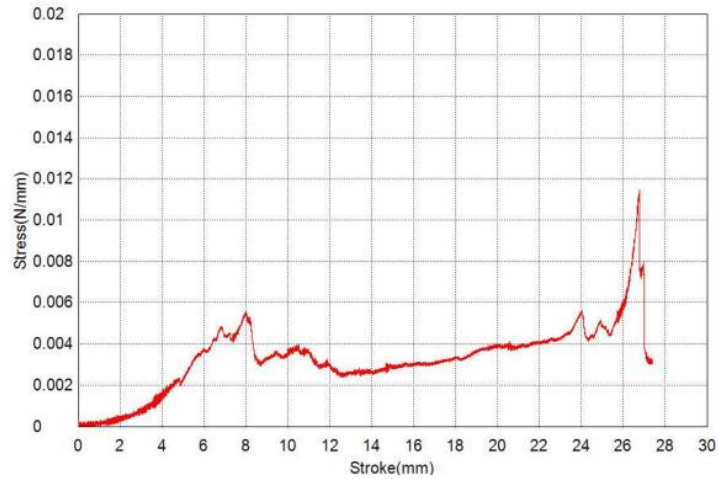


Figure 4.9: TPU Graph of 5µm GNP



Figure 4.10: TPU Graph of 15µm GNP

Figure 4.9 and 4.10 shows the graph of peel strength affected by the different GNP particle size between 5µm and 15µm. The peel strength of 5µm GNP was 0.00328 N/mm, while the peel strength of 15µm GNP was 0.00419 N/mm. Therefore, the GNP particle size of 15µm has a higher peel strength which has better adhesion compared to 5µm. The peel strength is also affected by the curing process parameters. As curing time and temperature were increased, the adhesion level increased rather quickly, resulting in higher adhesion properties. However, resistance will increase due to the over cure phenomena, in which some filler was burnt out. (Khirotdin et al., 2017)

CHAPTER 5

CONCLUSION AND RECOMMENDATION

5.1 Conclusion

Based on the results of the experiment, the mechanical and electrical effects obtained show that the reliability of this experimental set-up is unstable due to the high value of error. It is possible to conclude that some of the validations are unattainable owing to a variety of factors. Furthermore, the consistency result differed for each SCI sample, particularly when the formulation was made on separate days. When the sample is utilised numerous times for the cycle test, the bulk resistivity reading gradually increases. However, the goal of determining the maximum strain and acceptable strain was accomplished by doing a few experiments to obtain an average measurement. When the SCI sample was handled, it became extremely sensitive. When checked with a mulimeter, the bulk resistivity seems to become drastically inconsistent. Furthermore, when the peel strength is just subjected to varying particle sizes, it is difficult to interpret the results. The other variable must be included in order to evaluate further peel strength data. Further research in this area is recommended for a better understanding and implementation of the findings from this study.

5.2 Recommendation For Further Works

Several aspects of this project can still be developed and enhanced for future work. This study analyses two different particle sizes of GNP as filler materials in order to identify how different filler sizes might substantially affect SCI performance. Both particle size and the current work's positive dependability can be enhanced in future studies by attempting to modify new formulation or processing parameters to explore and examine more on SCI.

The cyclic stretch test's automatic jig must be set up and used to ensure uniformity in bulk resistivity values. This is crucial because the manual stretch test may face some challenges due to uneven force exerted to the ends of both sides, causing a few parts to shatter unexpectedly due to excessive force, which is the higher force concentrated at one point that causes it to rapidly fatigue.

A few cracks were also propagated due to the manual screen printing process, where the thickness was difficult to control, resulting in porosity in some areas after the curing process. Additionally, the uneven surface area results in unpredictability in the bulk resistivity. As a result, by utilising the inkjet printing method, it is possible to minimise human error caused by manual printing.

The peel test experiment also experienced difficulties due to the inconsistent value of peel strength due to the manual method of applying the epoxy between the glass slide and conductive ink. The minimal data obtained are typically inaccurate due to excessive ink. Therefore, the research needs to find an appropriate method that could avoid excessive epoxy when applied between two materials which are ink conductive filler and glass slides.

REFERENCES

Alemour, B., Yaacob, M. H., Lim, H. N., & Hassan, M. R. (2018). Review of electrical properties of graphene conductive composites. *International Journal of Nanoelectronics and Materials*, 11(4), 371–398.

AlMaadeed, M. A. A., Ponnamma, D., & El-Samak, A. A. (2020). Polymers to improve the world and lifestyle: physical, mechanical, and chemical needs. In *Polymer Science and Innovative Applications*. INC. <https://doi.org/10.1016/b978-0-12-816808-0.00001-9>

Anwar A. Mohammed, D. of P. (2017). *Development Of A New Stretchable And Screen Printable Conductive Ink*. 1–138.

Ashikin, A. S., Omar, G., Tamaldin, N., Kamarolzaman, A. A., Jasmee, S., & Ani, F. C. (2013). *Comparative Study on the Polyethylene Terephthalate (Pet) and Thermoplastic Polyurethane (Tpu) As Substrate Materials for Conductive Ink*. xx(January).

Ayatollahi, M. R., Shadlou, S., Shokrieh, M. M., & Chitsazzadeh, M. (2011). Effect of multi-walled carbon nanotube aspect ratio on mechanical and electrical properties of epoxy-based nanocomposites. *Polymer Testing*, 30(5), 548–556. <https://doi.org/10.1016/j.polymertesting.2011.04.008>

Capasso, A., Del Rio Castillo, A. E., Sun, H., Ansaldo, A., Pellegrini, V., & Bonaccorso, F. (2015). Ink-jet printing of graphene for flexible electronics: An environmentally-friendly approach. *Solid State Communications*, 224, 53–63. <https://doi.org/10.1016/j.ssc.2015.08.011>

Chatterjee, S., Nafezarefi, F., Tai, N. H., Schlagenhaut, L., & Nu, F. A. (2012). *Size and synergy effects of nanofiller hybrids including graphene nanoplatelets and carbon nanotubes in mechanical properties of epoxy composites*. 0, 1–7. <https://doi.org/10.1016/j.carbon.2012.07.021>

Cinquino, M., Prontera, C. T., Zizzari, A., Giuri, A., Pugliese, M., Giannuzzi, R., Monteduro, A. G., Carugati, M., Banfi, A., Carallo, S., Rizzo, A., Andretta, A., Dugnani, G., Gigli, G., & Maiorano, V. (2021). Effect of surface tension and drying time on inkjet-printed PEDOT:PSS for ITO-free OLED devices. *Journal of Science: Advanced Materials and Devices*. <https://doi.org/10.1016/j.jsamd.2021.09.001>

Coddet, P., Verdy, C., Coddet, C., & Debray, F. (2016). On the mechanical and electrical properties of copper-silver and copper-silver-zirconium alloys deposits manufactured by cold spray. *Materials Science and Engineering A*, 662, 72–79. <https://doi.org/10.1016/j.msea.2016.03.049>

Gao, J., Qu, R., Tang, B., Wang, C., Ma, Q., & Sun, C. (2011). Control of the aggregation behavior of silver nanoparticles in polyurethane matrix. *Journal of Nanoparticle Research*, 13(10), 5289–5299. <https://doi.org/10.1007/s11051-011-0515-8>

Hannila, E., Remes, K., Kurkela, T., Happonen, T., Keränen, K., & Fabritius, T. (2020). *The Effect of Torsional Bending on Reliability and Lifetime of Printed Silver Conductors*. 67(6), 2522–2528.

Hsu, C. P., Guo, R. H., Hua, C. C., Shih, C. L., Chen, W. T., & Chang, T. I. (2013). Effect of polymer binders in screen printing technique of silver pastes. *Journal of Polymer Research*, 20(10). <https://doi.org/10.1007/s10965-013-0277-3>

Htwe, Y. Z. N., Abdullah, M. K., & Mariatti, M. (2021). Optimization of graphene conductive ink using solvent exchange techniques for flexible electronics applications. *Synthetic Metals*, 274(April). <https://doi.org/10.1016/j.synthmet.2021.116719>

Huang, Y., Kormakov, S., He, X., Gao, X., Zheng, X., Liu, Y., Sun, J., & Wu, D. (2019). Conductive Polymer Composites from Renewable Resources: An Overview of Preparation, Properties, and Applications. *Polymersfile:///C:/Users/Muhammad Izwan/Desktop/JOURNAL PSM 2/Silver.Pdf*, 11(2), 1–32. <https://doi.org/10.3390/polym11020187>

Hung, M. T., Choi, O., Ju, Y. S., & Hahn, H. T. (2006). Heat conduction in graphite-nanoplatelet-reinforced polymer nanocomposites. *Applied Physics Letters*, 89(2), 0–3. <https://doi.org/10.1063/1.2221874>

Khirotidin, R. K., Hassan, N., Siang, H. H., & Zawahid, M. H. (2017). Printing and curing of conductive ink track on curvature substrate using fluid dispensing system and oven. *Engineering Letters*, 25(3), 336–341.

Lee, P., Lee, J., Lee, H., Yeo, J., Hong, S., Nam, K. H., Lee, D., Lee, S. S., & Ko, S. H. (2012). Highly stretchable and highly conductive metal electrode by very long metal nanowire percolation network. *Advanced Materials*, 24(25), 3326–3332. <https://doi.org/10.1002/adma.201200359>

Liu, Y., Xie, J., Liu, L., Fan, K., Zhang, Z., Chen, S., & Chen, S. (2021). Inkjet-printed highly conductive poly(3,4-ethylenedioxythiophene): Poly(styrenesulfonate) electrode for organic light-emitting diodes. *Micromachines*, 12(8). <https://doi.org/10.3390/mi12080889>

Merilampi, S., & Ruuskanen, P. (2009). Microelectronics Reliability The characterization of electrically conductive silver ink patterns on flexible substrates. *Microelectronics Reliability*, 49(7), 782–790. <https://doi.org/10.1016/j.microrel.2009.04.004>

Merilampi, Sari, Björninen, T., Haukka, V., Ruuskanen, P., Ukkonen, L., & Sydänheimo, L. (2011). Microelectronics Reliability Analysis of electrically conductive silver ink on stretchable substrates under tensile load. *Microelectronics Reliability*, 50(12), 2001–2011. <https://doi.org/10.1016/j.microrel.2010.06.011>

Mevold, A. H. H., Hsu, W. W., Hardiansyah, A., Huang, L. Y., Yang, M. C., Liu, T. Y., Chan, T. Y., Wang, K. S., Su, Y. A., Jeng, R. J., Wang, J. K., & Wang, Y. L. (2015). Fabrication of Gold Nanoparticles/Graphene-PDDA Nanohybrids for Bio-detection by SERS Nanotechnology. *Nanoscale Research Letters*, *10*(1), 1–7. <https://doi.org/10.1186/s11671-015-1101-2>

Mohammed, A., & Pecht, M. (2016). A stretchable and screen-printable conductive ink for stretchable electronics. *Applied Physics Letters*, *109*(18). <https://doi.org/10.1063/1.4965706>

Mou, Y., Zhang, Y., Cheng, H., Peng, Y., & Chen, M. (2018). Fabrication of highly conductive and flexible printed electronics by low temperature sintering reactive silver ink. *Applied Surface Science*, *459*(July), 249–256. <https://doi.org/10.1016/j.apsusc.2018.07.187>

Netnapa, E., Jaafar, M., Ahmad, Z., Ohtake, N., & Lila, B. (2017). Fabrication of PEDOT: PSS/graphene conductive ink printed on flexible substrate. *Solid State Phenomena*, *264* SSP(September), 70–73. <https://doi.org/10.4028/www.scientific.net/SSP.264.70>

Rogers, J. A., Someya, T., & Huang, Y. (2010). Materials and mechanics for stretchable electronics. *Science*, *327*(5973), 1603–1607. <https://doi.org/10.1126/science.1182383>

Romagnoli, M., Lassinantti Gualtieri, M., Cannio, M., Barbieri, F., & Giovanardi, R. (2016). Preparation of an aqueous graphitic ink for thermal drop-on-demand inkjet printing. *Materials Chemistry and Physics*, 182, 263–271. <https://doi.org/10.1016/j.matchemphys.2016.07.031>

Sun, Y., Mayers, B., & Xia, Y. (2003). Transformation of silver nanospheres into nanobelts and triangular nanoplates through a thermal process. *Nano Letters*, 3(5), 675–679. <https://doi.org/10.1021/nl034140t>

Vieroth, R., Löher, T., Seckel, M., Dils, C., Kallmayer, C., Reichl, H., & Allee, G. M. (2009). *Stretchable Circuit Board Technology and Application Stretchable Circuit Board Technology and Application*. September. <https://doi.org/10.1109/ISWC.2009.13>

Wang, D. Y., Chang, Y., Lu, Q. S., & Yang, Z. G. (2015). Nano-organic silver composite conductive ink for flexible printed circuit. *Materials Technology*, 30(1), 54–59. <https://doi.org/10.1179/1753555714Y.0000000204>

Wang, Q. W., Zhang, H. Bin, Liu, J., Zhao, S., Xie, X., Liu, L., Yang, R., Koratkar, N., & Yu, Z. Z. (2019). Multifunctional and Water-Resistant MXene-Decorated Polyester Textiles with Outstanding Electromagnetic Interference Shielding and Joule Heating Performances. *Advanced Functional Materials*, 29(7), 1–10. <https://doi.org/10.1002/adfm.201806819>

Wu, L., Hoa, S. V., Minh-Tan, & Ton-That. (2006). Effects of composition of hardener on the curing and aging for an epoxy resin system. *Journal of Applied Polymer Science*, 99(2), 580–588. <https://doi.org/10.1002/app.22493>

Yang, Y., Deng, H., & Fu, Q. (2020). Recent progress on PEDOT:PSS based polymer blends and composites for flexible electronics and thermoelectric devices. *Materials Chemistry Frontiers*, 4(11), 3130–3152. <https://doi.org/10.1039/d0qm00308e>

Yoo, D., Kim, J., & Kim, J. H. (2014). Direct synthesis of highly conductive poly(3,4-ethylenedioxythiophene):Poly(4-styrenesulfonate) (PEDOT:PSS)/graphene composites and their applications in energy harvesting systems. *Nano Research*, 7(5), 717–730. <https://doi.org/10.1007/s12274-014-0433-z>

Yoon, S. S., & Khang, D. Y. (2016). Roles of Nonionic Surfactant Additives in PEDOT:PSS Thin Films. *Journal of Physical Chemistry C*, 120(51), 29525–29532. <https://doi.org/10.1021/acs.jpcc.6b12043>